# DESIGN AND FABRICATION OF ANKLE FOOT ORTHOSIS UTILISING 3D SCANNER AND 3D PRINTING

**ONG YONG SHIEN**

**UNIVERSITI SAINS MALAYSIA**

**2021**

# DESIGN AND FABRICATION OF ANKLE FOOT ORTHOSIS UTILISING 3D SCANNER AND 3D PRINTING

By:

**ONG YONG SHIEN**

(Matrix number: 137860)

Supervisor:

**Assoc. Prof. Dr. Jamaluddin Abdullah**

July 2021

This dissertation is submitted to
Universiti Sains Malaysia
As partial fulfillment of the requirement to graduate with honors degree in
**BACHELOR OF ENGINEERING (MECHANICAL ENGINEERING)**

School of Mechanical Engineering
Engineering Campus
Universiti Sains Malaysia

# DECLARATION

This work has not previously been accepted in substance for any degree and is not being concurrently submitted in candidature for any degree.

Signed…………………………………………………… (Ong Yong Shien)

Date………………………………………………… (12/7/2021)

STATEMENT 1

This thesis is the result of my own investigations, except where otherwise stated.

Other sources are acknowledged by giving explicit references.

Bibliography/references are appended.

Signed…………………………………………………… (Ong Yong Shien)

Date………………………………………………… (12/7/2021)

STATEMENT 2

I hereby give consent for my thesis, if accepted, to be available for photocopying and for interlibrary loan, and for the title and summary to be made available outside organizations.

Signed…………………………………………………… (Ong Yong Shien)

Date………………………………………………… (12/7/2021)

# ACKNOWLEDGEMENT

# TABLE OF CONTENT

# LIST OF TABLES

# LIST OF FIGURES

# REKA BENTUK DAN FABRIKASI ORTHOSIS KAKI
# MEMANFAATKAN PENGIMBASAN 3D DAN PERCETAKAN 3D

## ABSTRAK

Dalam penyelidikan ini, dua jenis orthosis kaki iaitu *Solid AFO* dan *Free Motion AFO* telah direka bentuk dan dihasilkan dengan memanfaatkan teknik pengimbasan 3D dan pencetakan 3D. Perbezaan utama antara kedua-dua reka bentuk ialah *Solid AFO* terbuat dari satu bahagian padat. Bahagian belakang *Solid AFO* ditutup sepenuhnya dan tiada pergerakan pergelangan kaki dibenarkan. Untuk *Free Motion AFO*, ia dilengkapi dengan sendi lenturan yang membenarkan plantarflexion dan dorsiflexion di pergelangan kaki. Kajian ini dimulakan dengan proses pengimbasan 3D menggunakan *iPad* dan.sensor *Structure*. Beberapa proses perantaraan dilaksanakan seperti *mesh cleaning*, reka bentuk CAD, *slicing* dan penentukuran sebelum proses pencetakan 3D menggunakan *fused deposition modelling* (FDM). Kesan perbezaan antara orientasi model telah dikajikan. Empat orientasi yang dikajikan ialah merata, mendadar, 45 darjah tegak dengan sokongan normal dan 45 darjah tegak dengan sokongan pokok. Orientasi 45 darjah tegak dengan sokongan pokok dipilih sebagai orientasi optimum kerana penggunaan bahan (40 gram dan 13.44 meter) dan masa cetak (10 jam dan 36 minit) yang optimum, serta kualiti yang lebih baik. Kaedah unsur terhingga dilakukan untuk mengkaji tingkah laku reka bentuk di bawah beban statik dan dinamik. *Static structural analysis* dilakukan untuk mensimulasikan tingkah laku reka bentuk AFO dalam keadaan pemuatan statik hasil daripada daya tindak balas yang diberikan pada AFO oleh lantai. Sebaliknya, *transient structural analysis* dilakukan dengan mempertimbangkan kekuatan masa nyata yang diterapkan pada AFO pada sudut tibia yang berbeza pada empat tahap fasa pendirian.

# DESIGN AND FABRICATION OF ANKLE FOOT ORTHOSIS UTILIZING 3D SCANNER AND 3D PRINTING

## ABSTRACT

In this research, two types of AFOs which are Solid AFO and Free Motion AFO are designed and fabricated utilizing 3D scanning and 3D printing techniques. The major difference between the two designs is that Solid AFO is made of one solid part. The back of the Solid AFO is covered completely and thus allow no ankle motion. For Free Motion AFO, it is equipped with flexure joints which allows plantarflexion and dorsiflexion at the ankle. The process began with the 3D scanning process using an *iPad* and *Structure* sensor. Several intermediate processes are performed such as mesh cleaning, CAD design, slicing and calibrations before proceeding with 3D printing using fused deposition machining (FDM) printer. The part orientation is varied with four different orientations (flatwise, sidewise, 45 degrees upright with normal support and 45 degrees upright with tree support) and the performance of each orientation is studied. Orientation 4 (45 degrees upright with tree support) is selected as the optimum orientation due to the optimum material consumption (40 gram and 13.44 meters) and print time (10 hours and 36 minutes), as well as the outperform quality. Finite element analysis is performed to study the behaviour of the designs under static and dynamic loadings. Static structural analysis is performed to replicate the behaviour of the AFO designs under static loading conditions as the result of the ground reaction forces exerted on the AFO by the ground. On the other hand, transient structural analysis is performed by considering the real-time force applied to the AFO at different tibia angles with respect to four stages of the stance phase (loading response stage, mid-stance stage, terminal stance stage and pre-swing stage).

# CHAPTER 1

# INTRODUCTION

## 1.1    GENERAL INTRODUCTION

Foot drop is a medical condition in which the patient is unable to lift the forefoot. This causes involuntary plantarflexion and results in restriction in the range of movement at the ankle. The main cause of foot drop is the injury of the peroneal nerve which controls the muscles movement involved in lifting the foot. Another cause of foot drop is musculoskeletal disorders and neuromuscular diseases such as amyotrophic lateral sclerosis (ALS), peripheral neuropathy, polio and cerebral palsy (CP) which causes progressive muscle weakness.

One of the treatments of foot drop is wearing an Ankle Foot Orthosis. (AFO). AFO is a splint that is designed to realign and maintain the feet and ankles in a normal position. AFO also helps to provide support to the patients' feet to promote dorsiflexion of feet, restrict and reduce the movements at the ankle, provide protections to the ankle and improve gait performance. Due to the diversity of the AFO, AFO can be different in terms of the materials, shape, strength, size and functionality. Some examples of AFO are dynamic AFO, solid AFO, posterior leaf spring AFO, ground reaction AFO and hinged AFO.



Figure 1.1      Illustration of foot drop [1].
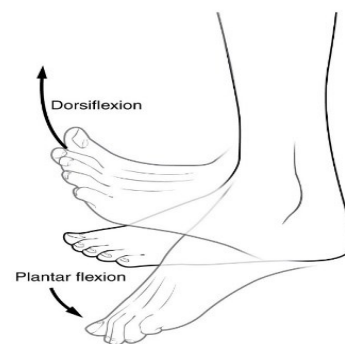
Figure 1.2      Illustration of dorsiflexion and plantarflexion [2].

The conventional manufacturing process of AFO involves the creation of the positive mold using the plaster-mold casting process. The mold is then used as the reference to form the AFO through thermoforming of polymers. However, due to the advancement in rapid prototyping technologies, the manufacturing process has been transitioned to the rapid prototyping process, or additive manufacturing process to be exact. The utilization of 3D scanners together with the additive manufacturing process has the potential to become the future trend of AFO manufacturing.

## 1.2    PROJECT BACKGROUND

The conventional manufacturing process involves thermoforming of plastics. Thermoforming is a process for forming thermoplastic sheets or films over a mold through the application of heat and pressure (Kalpakjian, Schmid, and Musa 2009). First, the mold is produced by plaster-mold casting. The plaster slurry (mixture of gypsum/calcium sulphate, talc, silica flour and water) is poured and wrapped around the patient's limb. After the plaster slurry set, the patient's limb is removed and leaving the plaster mold. The plaster mold is further dried at a higher temperature (typically between 120°C to 260°C, although a higher temperature drying temperature is possible, depending on the type of plaster). After that, trim lines are drawn on the mold according to the desired shape. Next, thermoforming of plastics takes place. A plastic sheet is clamped and heated to a sag point (above the glass-transition temperature of polymer). Then, the plastic sheet is forced against the mold surfaces through the application of a vacuum. A raw AFO is formed. Lastly, the AFO is trimmed according to the trim lines that were drawn previously.
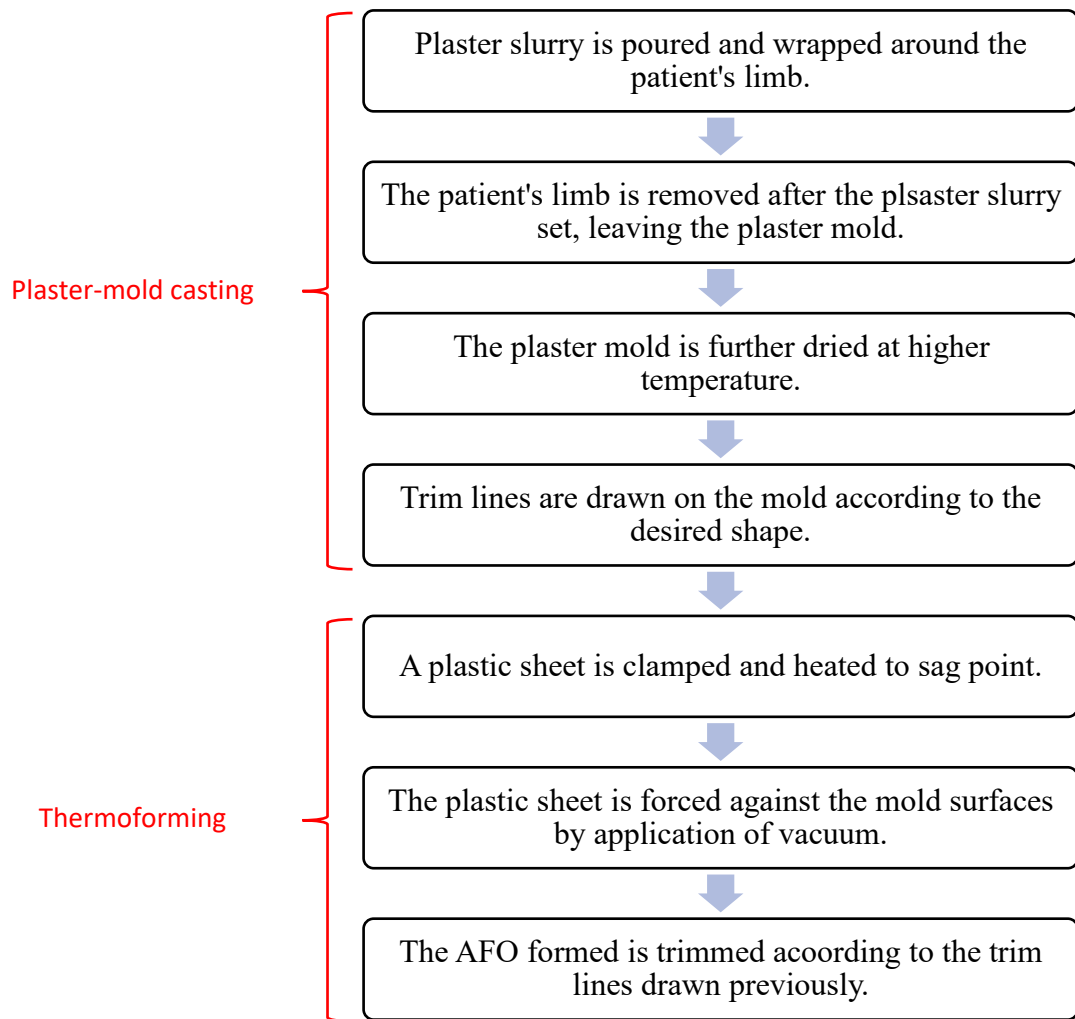
Figure 1.3　Process flow to manufacture AFO using conventional manufacturing process.

However, the main drawback of manufacturing AFO using the conventional manufacturing process is the long lead time. Due to the complexity of the conventional manufacturing process, the process is time-consuming and reliance on delicate skills. Thus, new technologies needed to be implemented to improve the productivity and quality of AFO.

As mentioned in the title of this project, the focus of this project is to utilize 3D scanning and 3D printing technologies in the design and fabrication of ankle foot orthoses (AFO). 3D scanning technology integrated with CAD software scans the foot anatomy and converts it to the "STL" file before proceeding to 3D printing. The

scanning is instantaneous and will produce a real-time image of the patient's foot. Besides, the CAD can be modified quickly and easily with the aids of CAD software, thus reducing the lead time. To further increase productivity and reduce the lead time of the manufacturing of AFO, rapid prototyping is introduced. Additive manufacturing is one of the categories of the rapid prototype. Additive manufacturing is the manufacturing process in which the product produced by building it up through incremental addition of material. One of the examples of additive manufacturing is fused filament fabrication, or known as 3D printing. With the implementation of 3D scanning and 3D printing in manufacturing, the lead time can be significantly reduced.

## 1.3    PROBLEM STATEMENT

AFO can be separated into two types: prefabricated and customized. Also known as "off-the-shelf" AFO, the prefabricated usually have various types and sizes. The prefabricated AFO can be modified and adjusted to produce the best fitting AFO in terms of comfort and functionality, given that it is not constructed from a customized mold that is based on the patient's anatomy. However, such modifications and adjustments required delicate skills and have low flexibility, which means the AFO needed to be rebuilt if there is any error/mistake. On the other hand, a customized AFO requires a customized mold according to the patient's anatomy. However, the main drawback of customized AFO is the long lead time. The manufacturing process of customized AFO is time-intensive and thus lead to a long lead time. Another issue with customized AFO is that there is some level of material wastage. This is because the customized mold cannot be reused. Furthermore, there are also waste during the trimming and shaping process.

However, utilizing the 3D scanning technology and additive manufacturing process such as 3D printing, the designing process has higher flexibility. The design or the CAD can be modified and adjusted easily in the CAD software before fabrication. Apart from that, the latest technologies are higher in terms of efficiency and productivity. The lead time is shorter compared to the conventional manufacturing process besides having a longer operating time compared to human labour since the 3D printer can operate twenty-four hours a day, seven days a week. Moreover, another advantage of the 3D printing process is that it produces less waste since it is an additive manufacturing process, in which the AFO is built up by overlapping layers of material incrementally.

## 1.4    OBJECTIVES

The objectives of this project are:

i.    To study, design and fabricate AFO that is suitable for local use in Malaysia by utilizing the latest development in technology such as the 3D scanner and 3D printing.

ii.    To study and evaluate the performance of the AFO fabricated through finite element analysis.

## 1.5    PROJECT SCOPES

The scope of work in this project involves:

i.    Obtain the patient's foot anatomy using the 3D scanner and transform it into readable data in CAD software.

ii.  Design a customized AFO based on the scanned data with the aids of CAD software.

iii.  Fabricate a customized AFO utilizing 3D printing technology.

iv.  Perform finite element analysis to simulate the behaviour of the AFO under loading conditions.

# CHAPTER 2

# LITERATURE REVIEW

## 2.1 AFO FABRICATION UTILIZING 3D SCANNING TECHNOLOGY INTEGRATED WITH ORTHOSIS SOFTWARE AND 3D PRINTING TECHNOLOGY

According to the research published by Yong Ho Cha et al, an AFO is successfully fabricated utilizing Artec$^{TM}$ Eva 3D scanner by Artec Group, Luxembourg which is then integrated with orthosis software, MediACE3D$^{®}$ by SolidEng Corp., Daejeon, Korea to generate the "STL" file before it is printed using FB 9600® Fused Filament Fabrication type 3D printer by TPC Mechatronics Corp., Incheon, Korea [3]. In the research, mechanical stress tests were performed to evaluate the durability of the 3D printed AFO. A stretching force of 50N is applied, representing the partial body weight applied on the AFO, with sine waves of 1Hz frequency, simulating the cadence of walking. The test was repeated for 300,000 cycles, representing 4 months of activity by the patient, with an assumption of 2,500 steps per day. The results of the stress test showing that there was neither crack nor damage after the test and the shape and stiffness of the 3D printed AFO remains the same. Besides, gait analysis was performed to evaluate the performance of conventional AFO and 3D printed AFO apply to real patients. Based on the gait analysis results, the gait speed increased from 42.2cm/sec to 56.5cm/sec after wearing conventional AFO and 56.5cm/sec after wearing 3D printed AFO. The stride length increased after wearing the conventional AFO (70.9 cm) and 3D-printed AFO (70.9 cm) compared to that without an AFO (63.2 cm). Apart from that, kinematic and dynamic electromyography analyses were carried out using 3D gait analysis, HWK-200RT$^{®}$ by Motion Analysis Corp., USA. The result of the kinetic analysis shows that in the swing phase, dorsiflexion is more obvious after using

conventional AFO followed by 3D printed AFO and the case without an AFO. The foot rotation has the highest level of correction after wearing conventional AFO, followed by 3D printed AFO and without an AFO. Whereas for ankle eversion, the level of correction for both conventional and 3D printed AFO is about the same.
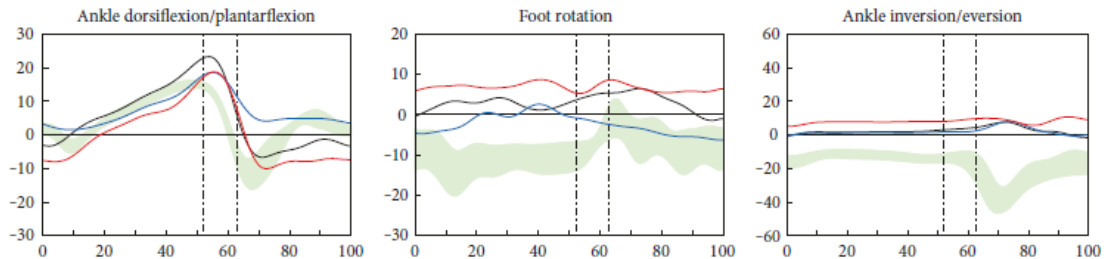


Figure 2.1    Ankle dorsiflexion/plantarflexion, foot rotation and ankle inversion/eversion of conventional AFO (blue line), 3D-printed AFO (black line) and without AFO (red line) [3].

## 2.2    CONVENTIONAL MANUFACTURING PROCESS VERSUS ADDITIVE MANUFACTURING PROCESS

The conventional manufacturing (CM) and additive manufacturing (AM) of AFO was compared by F. S. Shahar et al [4]. According to the results, one of the advantages of AM over CM is shorter production time. A research was done by researchers at Gonzaga University to compare the traditional AFO and 3D printed AFO. From their findings, the production time of AFO can be significantly reduced from four weeks to two days after implementing 3D printing. Farah Syazwani Shahar compares the strength and stiffness of conventional AFO and 3D printed AFO based on the tests done by other researchers. From the results, she claims that the tensile strength and Young's Modulus of the AFO produced by AM and CM is similar. However, AM can significantly reduce the production time, besides having a simpler manufacturing method. This shows that the AM will not compromise the original strength achieved by CM thus proving AM to be more beneficial compared to CM.

| Types of Material | Tensile Strength (MPa) | Young's Modulus (GPa) | Fabrication Method | Material Cost (RM/kg) | Material Characteristics |
|---|---|---|---|---|---|
| ABS | 25.390 | 1.325 | FDM (AM) | 57.75–111.37 | • No warping during 3D printing<br>• High impact resistant |
| ABS | 29.600 | 1.790 | Thermoformed polymer (CM) | 184.64–637.25 | • Excellent chemical, stress, and creep resistance<br>• Food grade thermoplastic<br>• Excellent fire and heat resistant<br>• Recyclable |
| PLA | 42.660 | 3.930 | FDM (AM) | 61.87–111.37 | • Minimal warping during 3D printing<br>• Odourless when used in 3D printing<br>• Eco-friendly (derived from corn starch or sugar cane)<br>• Biodegradable |
| PP | 20.040 | 1.508 | FDM (AM) | 251.68–503.35 | • High warping during 3D printing<br>• Chemical resistant |
| PP | 20.000 | 1.000 | Thermoformed polymer (CM) | 40.40–1757.00 | • Flexible<br>• Lightweight<br>• FDA approved |
| PETG | 34.140 | 2.270 | FDM (AM) | 66.00–198.00 | • No warping during 3D printing<br>• Extremely durable and odourless |
| PETG | 50.000 | 1.900 | Thermoformed polymer (CM) | 178.58–3066.56 | • High impact resistant<br>• Water, chemical, and fatigue resistant |
| Nylon | 34.790 | 0.073 | FDM (AM) | 206.25–319.87 | • Low odour when used in 3D printing<br>• Strong<br>• Lightweight<br>• Durable<br>• Flexible<br>• Mechanical stability and hardness<br>• High fatigue resistance<br>• FDA approved |

Figure 2.2        Comparison between CM and AM properties and material characteristics [4].

## 2.3    SMART INSOLE ON REAL-WORLD STEP COUNT

One of the objectives of this project is to produce an AFO with tracking ability. This can be done by integrating measuring systems into the AFO. Some information such as the daily step count can be an important parameter to evaluate the performance of a patient wearing an AFO in order to provide a more specific treatment or rehabilitation. Thus, step count is one of the main and important features in an AFO. In the research done by the researchers from University at Buffalo, SUNY Buffalo, New York and Shenzhen Chuanggan Technology (Sennotech), Shenzhen, China, the researchers implemented a smart insole system design and evaluated the step count performance [5]. The smart insole has the advantages of a lightweight, thin and convenient to use, which is suitable to be installed on the AFO. The concept behind the

step count of the smart insole is based on the differential value threshold of the average plantar pressure obtained from the ambulatory gait assessment. The performance of the smart insole was evaluated by the researchers by performing a set of real-world experiments based on different circumstances. The results show that the smart insole system developed by the researchers is able to achieve nearly 100% accuracy in counting steps under different circumstances. The smart insole consists of pressure sensors array and inertial measurement unit (IMU) sensors, ultra-low power micro control unit (MCU) and Bluetooth Low Energy (BLE) wireless transmission module, a channel multiplexer (MUX), a Li-battery, and a micro-Universal Serial Bus (USB) connector module.
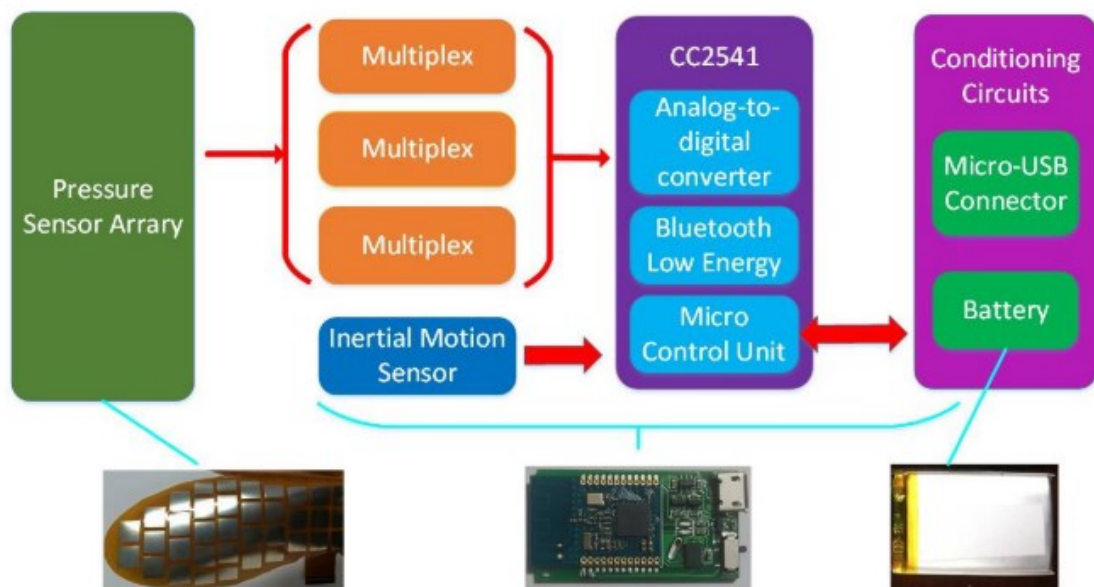


Figure 2.3      The overall architecture design for Smart Insole and pictures for each component [5].

## 2.4    3D PRINTERS

There are two 3D printers involved in this research, which are the *Creality Ender 3* and *Creatbot D600 Pro*.

*Creality Ender3* is an open-source 3D printer with high printing precision at an affordable price. It is a fused deposition modelling (FDM) type printer for small scale projects due to the small print space. It has a working envelop of 220 × 220 × 250 mm. The maximum allowable printing speed is 180 mm/s with various filaments of 1.75mm such as PLA, TPU, ABS and more. The G-code can be imported to the machine through SD cards or online The allowable layer thickness is ranged between 0.1 mm to 0.4 mm. It has a nozzle diameter of 0.4mm with a printing accuracy of ±0.1 mm. The maximum temperature where the nozzle can reach up to is 255 degrees Celsius and it is equipped with a hotbed with a maximum temperature of 110 degrees Celsius.



Figure 2.4    *Creality Ender 3* FDM printer [6].

On the other hand for *Creatbot D600 Pro*, has a fully enclosed print volume of 600 × 600 × 600 mm which allows large scale parts to be printed with this machine. The fully enclosed chamber isolates the printing parts from the impurities in the surrounding. The HEPA air filter absorbs impurities and fumes produced during the printing process, make the machine safer to be used. Inside the enclosed chamber, it is

equipped with a heating element to control and maintain a constant temperature inside the chamber to reduce the deformation of the part. Apart from the hot air chamber, *Creatbot D600 Pro* printer a filament drying room to provide dry storage especially for hygroscopic filaments like Nylon, PC, ABS and others. The *Creatbot D600 Pro* printer has two nozzles with a maximum nozzle temperature of 260 degrees Celsius and 420 degrees Celsius respectively. The printer supports dual-head printing with the two nozzles equipped. Due to the high allowable nozzle temperature, many materials can be printed using *Creatbot D600 Pro* printer, namely PLA, TPU, ABS, PETG, PC, Carbon Fibre, PEEK and more. It has a nozzle diameter of 0.4 mm and a precision of 0.5 mm with a maximum printing speed of up to 200 mm/s. It has an auto bed levelling (ABL) system with the BLTouch semiconductor hall sensor, which makes the bed levelling process much easier.



Figure 2.5      *Creatbot D600 Pro* 3D printer [7].

## 2.5    EFFECTS OF PART ORIENTATION

Part orientation defines the arrangement of the part in terms of the rotation in the work envelope around the coordinate system of the machine. Part orientation is one of the printing parameters that should take into considerations before the rapid prototyping process as many aspects were influenced by part orientation, such as strength, quality, surface finish, level of details, material consumption and most importantly printing time.

Parts made of FDM inherit anisotropic properties, which means the strength of the part is depending on the direction. More specifically, it has better strength in the XY direction than the Z direction [8]. Since in FDM, the parts are built by depositing materials layers by layers in the direction of the Z-axis. It has a higher probability for the part to fracture when forces are applied in the Z direction due to layer separation and poor bonding between layers. Thus, it is important to consider the application of the part and the direction of load in the part orientation during the rapid prototyping process. The rule of thumb is that the load should always parallel to the direction of the layers built up. Bellini and Güçeri [9] experimentally examined the tensile strength and Young's modulus of six-dog bone specimens built with ABS at different orientations as shown in Figure 2.7. From the result, the specimen that is built in XZ-orientation has the lowest tensile strength among the orthogonally built specimens, which is 7.608 MPa and Young's modulus of 1391.448 MPa. Whereas YZ-oriented specimen exhibits the highest tensile strength and Young's modulus, which is 15.987 MPa and 1652.523 MPa respectively. This is because, for the XZ-oriented specimen, the tension force is parallel to the building direction where the interlayer bonding is the weakest and usually where defects occur. The result of the tensile test is shown in Figure 2.8.
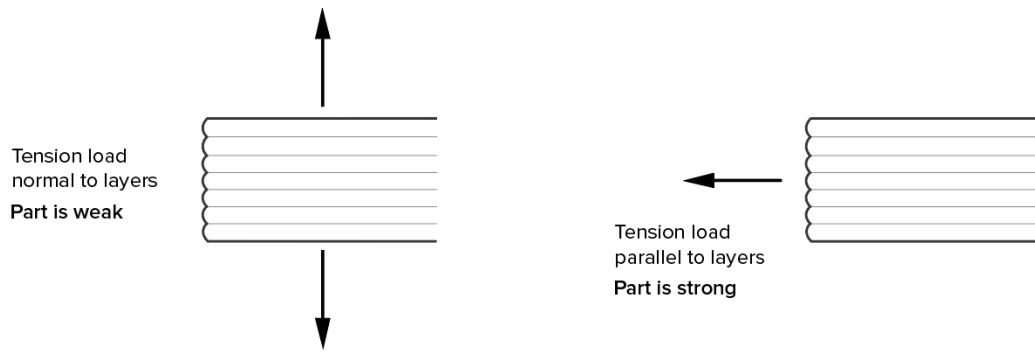
Figure 2.6    Illustration of how the strength is affected by part orientation and the direction of load applied.
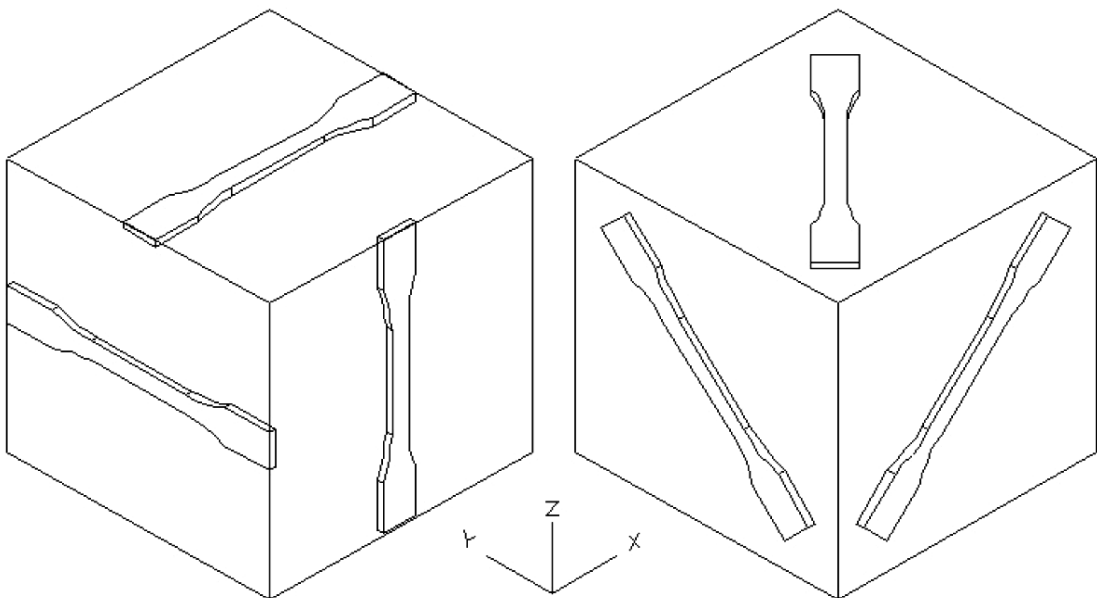


Figure 2.7    Orientation of the specimens in the experiment by Bellini and Güçeri [9].

| Toolpath | Build plane | Orientation | Number of specimens tested | Number of specimens considered | Tensile strength (MPa) | Elastic modulus (MPa) |
|---|---|---|---|---|---|---|
| [0 90 +45 −45] | xy | X | 4 | 4 | 11.700 | 1072.900 |
| [0 90 +45 −45] | yz | Y | 4 | 4 | 15.987 | 1652.523 |
| [0 90 +45 −45] | xz | Z | 11 | 6 | 7.608 | 1391.448 |
| [0 90 +45 −45] | xy | x + 45 | 5 | 5 | 10.808 | 970.944 |
| [0 90 +45 −45] | yz | y + 45 | 5 | 4 | 13.465 | 1519.115 |
| [0 90 +45 −45] | xz | z + 45 | 3 | 3 | 14.702 | 1527.600 |

Figure 2.8    Tensile test result by Bellini and Güçeri [9].

Despite the strength, the surface finish and level of details of a 3D printed part are affected by part orientation as well. In FDM, support is required in printing parts

that have high complexity and overhangs. Some details will be lost while removing the support structures. Generally, the top surfaces of the FDM printed part will have the highest level of details and thus have the best surface finishing as there is no support structure attached to it. Thus, the face which required a high level of detail should always face upwards.

The material consumption and printing time of the FDM process can be influenced by many factors, such as part orientation, type of build plate adhesion, type of support, layer height and others. The material consumption and printing time are proportional to the amount of support structures required. Parts with more support structures require more material and time to print. However, it can be compensated by optimizing the part orientation during printing. In the research by Tanoto et al [10], three dog bone specimens were produced at different orientations with raft build plate adhesion to investigate the influence of object orientation on the processing time. The variation of the object orientations is shown in Figure 2.9. The processing time for the third orientation is the shortest, which is 2432 s. This is because the support structure is not required in this orientation and the area of the raft base is the smallest. Whereas for second orientation, it requires the longest processing time, which is 2780 s. The result is shown in Figure 2.10. The reason for which the second orientation recorded the longest processing time is that it contains overhangs and required the highest amount of support structure. Apart from that, it has a wider area of raft base compared to the third orientation.
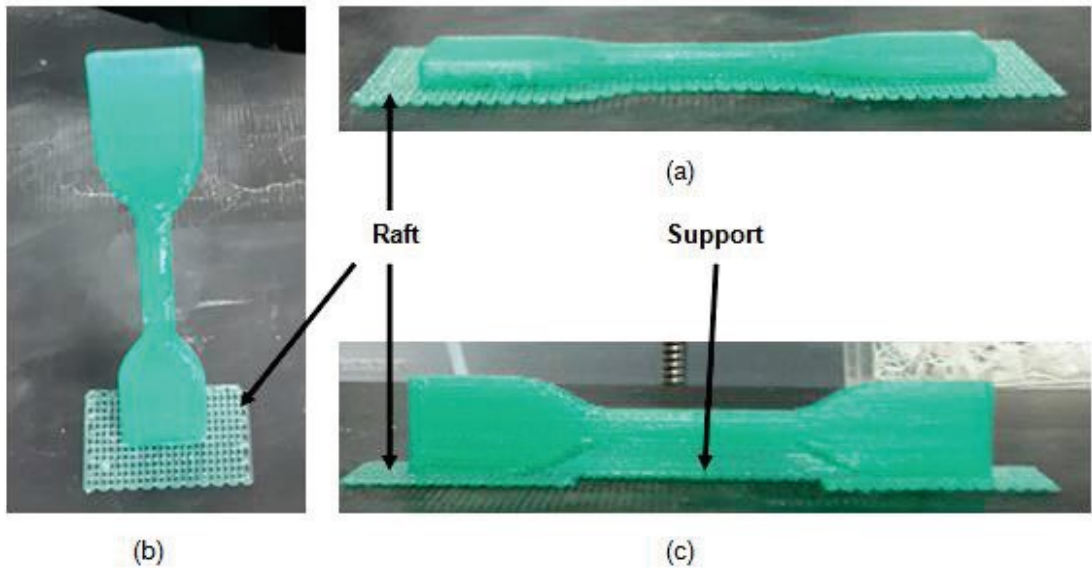
Figure 2.9    Raft and Support in Specimen at (a) First Orientation (b) Third
Orientation (c) Second Orientation [10].
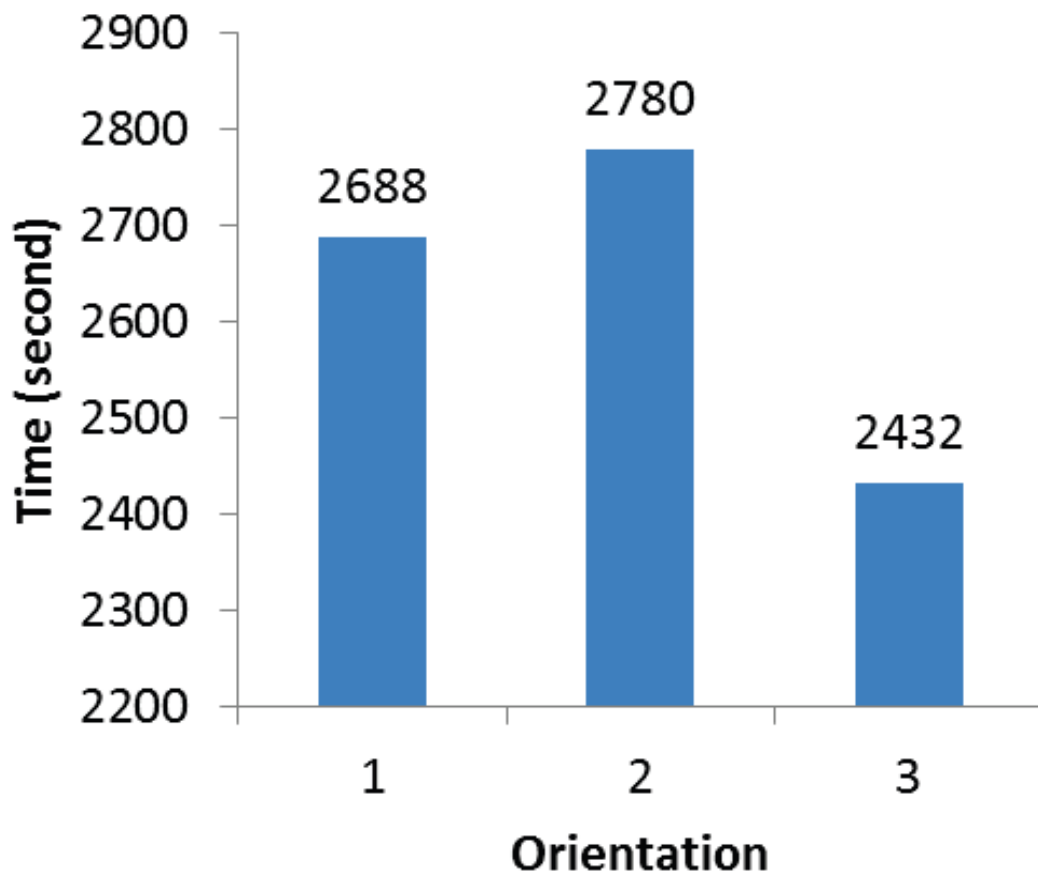


Figure 2.10    Processing time of the specimens at different orientations [10].

## 2.6    TYPE OF AFO DESIGNS

Table 2.1    Type of AFO designs.

| | Dynamic AFO | Solid AFO | Posterior Leaf Spring AFO | Ground Reaction AFO (GRAFO) | Hinged AFO |
|---|---|---|---|---|---|
| Type of AFO |  Dynamic AFO. |  Solid AFO. |  Posterior Leaf Spring AFO. |  Ground Reaction AFO (GRAFO). |  Hinged AFO. |
| Description | It should only be used where there are coronal or transverse plane deformities of the foot and ankle that can be passively corrected with minimal force. | It allows no ankle motion. It covers the back of the leg completely and extends from just below the fibular head to metatarsal heads. | It is a rigid AFO trimmed behind the malleoli bone to provide flexibility at the ankle and allows passive ankle dorsiflexion during the stance phase. | Made with a solid ankle, the upper portion wraps around the anterior part of the tibia proximally with a solid front over the tibia. The rigid front provides strong ground reaction support for patients with weak triceps surae. | It has a mechanical ankle joint usually preventing plantar flexion, but allowing relatively full dorsiflexion. It permits dorsiflexion in stance phase of the gait, thus making it easier to walk on uneven surfaces and stairs. |

# CHAPTER 3

# RESEARCH METHODOLOGY

## 3.1 OVERALL FLOW CHART

The processes involved in the fabrication of AFO are 3D scanning, mesh cleaning, CAD design, conversion to STL format, slicing, rapid prototyping and post-processing. The overall design and fabrication workflow is shown in Figure 3.1.

```
┌─────────────────────────────┐
│         3D scanning         │
└─────────────────────────────┘
              ▼
┌─────────────────────────────┐
│        Mesh cleaning        │
└─────────────────────────────┘
              ▼
┌─────────────────────────────┐
│         CAD Design          │
└─────────────────────────────┘
              ▼
┌─────────────────────────────┐
│        Import to STL        │
└─────────────────────────────┘
              ▼
┌─────────────────────────────┐
│           Slicing           │
└─────────────────────────────┘
              ▼
┌─────────────────────────────┐
│ Rapid prototyping (3D Printing) │
└─────────────────────────────┘
              ▼
┌─────────────────────────────┐
│       Post-processing       │
└─────────────────────────────┘
```
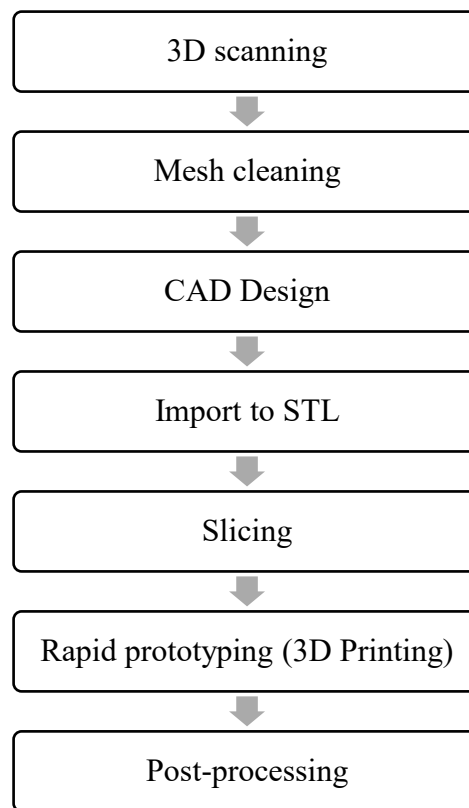
Figure 3.1     Overall process flowchart of AFO fabrication.

## 3.2 PROCESS BREAKDOWN

## 3.2.1 3D SCANNING PROCESS

In this research, the 3D scanning process is performed utilizing *Structure* by *Occipital, Inc.* [11]. The *Sructure* system requires two major components, which are *iPad* and *Structure sensor*. *Structure sensor* is a depth sensor that contains a frequency-

matched infrared structure light projector and a camera. It allows distances to be calculated accurately with reference to the distance between them. Infrared light passed through a diffraction grating and a speckle pattern is projected onto the environment by the infrared structure light projector. The reflected infrared light is captured by the infrared camera and depth data are generated and mapped with the aids of the accelerometer and gyroscope equipped in the *iPad*. The main advantage of the *Structure* system is that the 3D scanning system is portable, which is convenient, especially for the impaired patients.

The depth data generated needs to be post-processed in order to create a mesh. The platform used is the open-source *Scanner* sample app in the *Structure SDK*. To begin the scanning process, the *Structure sensor* is connected to the *iPad* using a lightning cable. After the *Scanner* app is launched, the size of the transparent cube (region of interest) is adjusted so that the object is bounded by the transparent cube. The *iPad* with *Structure sensor* is panned around the object to capture complete depth data to create a mesh. For a better-quality scan, the object should be located at the center of the scanner's panning path with a radius of approximately 1 meter. Apart from that, the speed of panning around the object should be consistent to ensure the object maintains in track. It is also important to ensure the 360º panning path around the object remains unimpeded to ease the mesh cleaning process. After a complete mesh is generated, the mesh file is exported to .OBJ file.



Figure 3.2      Image of Structure sensor connected to iPad [12].



Figure 3.3      Scanning process of the foot and the display in *Scanner* app platform [13].

### 3.2.2 MESH CLEANING AND PREPROCESSING PROCESS

After the mesh is created from the 3D scanning platform, the mesh may contain noises that need to be removed before proceeding with CAD design. The main purposes of mesh cleaning include removing noises, identify and fill holes, smoothing and refining mesh. In this research, the software used for mesh cleaning and preprocessing is *Meshmixer* by *Autodesk* [14].
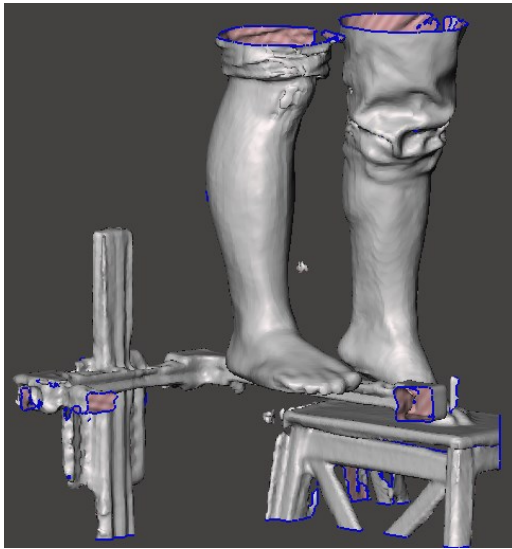


Figure 3.4      Mesh of the foot imported from raw scanned data.

Figure 3.5      Mesh of the foot after removing noises.

Figure 3.4 shows the mesh of the foot imported from raw scanned data. As shown in Figure 3.4, the mesh contains noises and holes which need to be eliminated and filled. To remove the noises, the region of interest is first selected, and the selection is expanded to regions connected to it. Then, the noises are selected by inverting the previous selection. The noises are then discarded. Next, a plane cut is applied to remove the excess part. Figure 3.5 shows the mesh of the foot after noises were removed. After noises removal, the mesh needs to be repaired by filling the holes and smoothing the mesh.
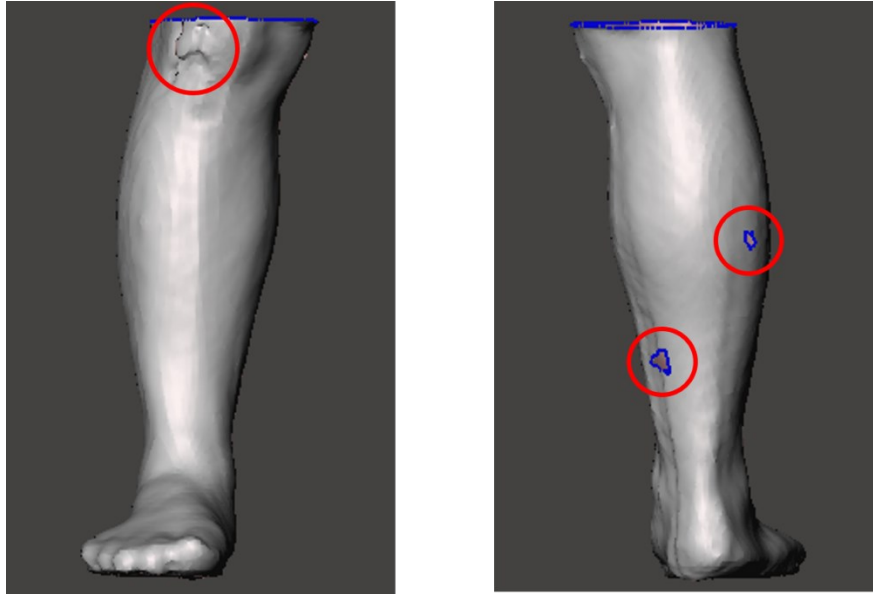
Figure 3.6      Defects of 3D scanning process resulted in the mesh of the foot.

As shown in Figure 3.6, there are some holes and overlapping surfaces as a result of the 3D scanning process defects. To produce a quality mesh, the holes are filled and the overlapping surfaces are discarded then filled. After all, the mesh is filled to generate a solid body. Lastly, the surface of the solid body is smoothed by refining the mesh. The solid body of the scanned foot after mesh cleaning is shown in Figure 3.7.



Figure 3.7      Results of mesh cleaning.

### 3.2.3    AFO CAD DESIGN

The AFO is designed using MediACE3D software by RealDimension Inc [15]. MediACE3D a 3D CAD software that is specifically for the design of custom 3D

printed orthosis in the field of orthopaedics and rehabilitation. The processes involved in CAD design using MediACE3D software is shown in Figure 3.8.

```
┌─────────────────────────────┐
│    Import 3D scanned model   │
└─────────────────────────────┘
              ⬇
┌─────────────────────────────┐
│       Skeleton creation      │
└─────────────────────────────┘
              ⬇
┌─────────────────────────────┐
│   Foot posture rectification │
└─────────────────────────────┘
              ⬇
┌─────────────────────────────┐
│   AFO CAD design with template│
└─────────────────────────────┘
              ⬇
┌─────────────────────────────┐
│      Refinement of design    │
└─────────────────────────────┘
              ⬇
┌─────────────────────────────┐
│     Export CAD design to stl │
└─────────────────────────────┘
```
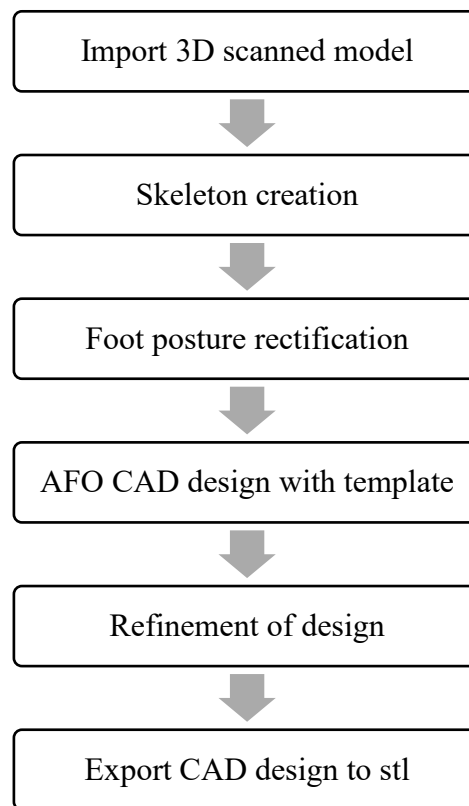
Figure 3.8      Flowchart of processes involved in CAD design using *MediACE3D*.

The refined 3D scanned data is first imported to the workspace in *MediACE3D*. Fifteen foot indices are selected and marked manually. A skeleton will be constructed and a foot analysis report generated, which contains the measurement of the critical dimensions of the scanned foot based on the foot indices selected. The example of the foot analysis report is shown in Figure 3.9. The report contains important dimensions of the patient's foot such as the medial malleolus height, lateral malleolus height, foot breadth instep height and foot length.

# Foot Analysis Report



**Foot Point Index List**

A : Heel Center
B : Lateral forefoot Center
C : Medial forefoot Center
D : 1st Metatarsophalangeal
  Medial border (1st MTP Medial border)
E : Navicular Tuberosity
F : Medial malleolus center
G : Calcaneal tuberosity Center
H : Lateral Malleolus Center
I : Styloid Process Lateral Center Point

J : 5th Metatarsophalangeal
  lateral border (5th MTP lateral border)
K : Head of 2nd Metatarsal
L : 2nd Toe Front End Point
M : Tibial tuberosity
N : Medial Epicondyle Center
O : Lateral Epicondyle Center
① : Highest Point of Instep Circumference
② : Ankle Center (F-H Mid Plantar Point)
③ : Knee Joint Center (N-O Mid Point)
④ : Medial Malleolus Center

**Foot Measure List**

| Foot Measure Items | | L | R | Foot Measure Items | L | R |
|---|---|---|---|---|---|---|
| Medial Longitudinal | 1 : LAA | | 135.9 | 11 : Lateral Malleolus Height | | 79.3 |
| Arch (MLA) | 2 : MLAA | | 145.8 | 12 : Instep Length 50% of Foot Length | | 129.5 |
| 3 : Resting Calcaneal Stance Position Angle | | | -19.7 | 13 : 1st MTPJ Frontal Length | | 56.9 |
| 4 : Tibial Mechanical Axis Angle | | | 7.6 | 14 : 5th MTPJ Frontal Length | | 80.2 |
| 5 : Metatarsal Angle | | | 101.6 | 15 : Foot Length | | 259.0 |
| 6 : Transverse Arch Angle | | | 115.4 | 16 : 1st MTPJ Length | | 202.0 |
| 7 : Calcaneus Length | | | 111.1 | 17 : 5th MTPJ Length | | 178.8 |
| 8 : Navicular Tuberosity Height | | | 42.1 | 18 : Metatarsal  Length | | 115.4 |
| 9 : Medial Malleolus Height | | | 98.7 | 19 : Foot  Breadth Instep Height | | 113.1 |

Figure 3.9     Foot analysis report generated in *MediACE3D* software based on the foot indices marked manually.

The foot posture of the scanned foot can be rectified by adjusting the flexion and eversion angle at the subtalar and talocrural joint. This step is important to compensate for any distortion of the foot during the scanning process.  The result of before and after rectification is shown in Figure 3.10 to Figure 3.13.
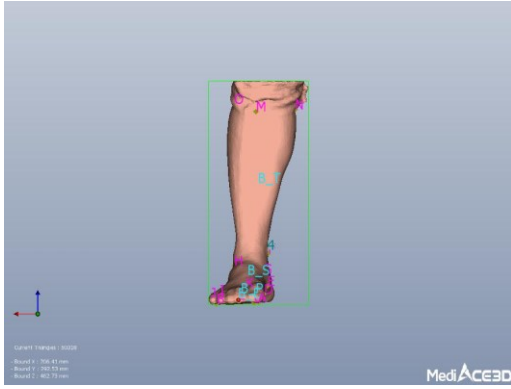
Figure 3.10     Front view of the
scanned foot before rectification.
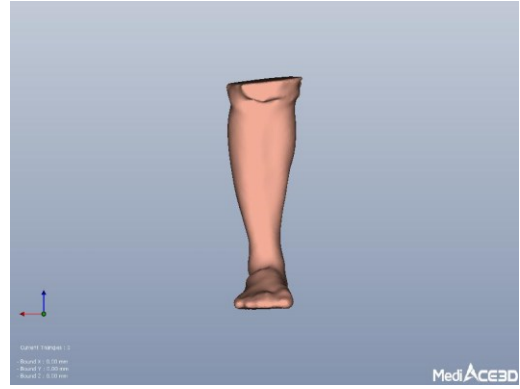


Figure 3.11     Front view of the foot
after rectification.
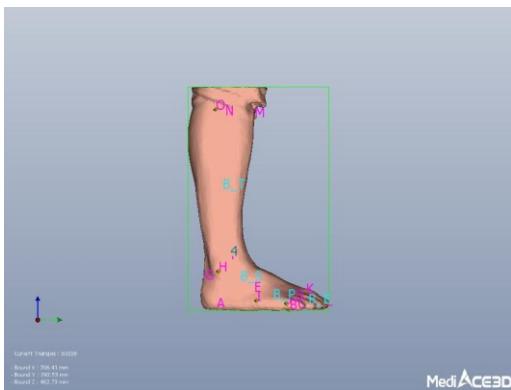


Figure 3.12     Side view of the
scanned foot before rectification.
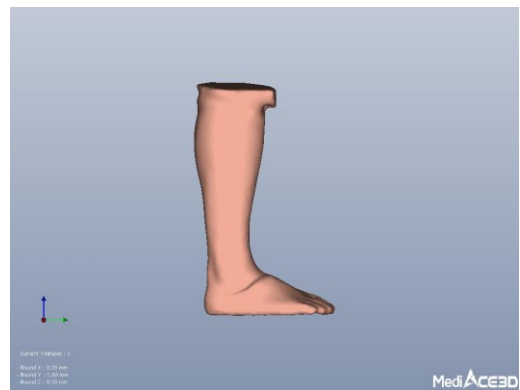


Figure 3.13     Side view of the
scanned foot after rectification.

After rectification, the programmed AFO template design is applied with size modified based on the foot indices selected previously. The template design is modified to suit the size of the foot better. The AFO design is imported to STL format and is further processed in *SolidWorks* to add on the cavity for strap attachment and perforated holes for better ventilation.

In this research, two designs are generated, which are solid AFO and free motion AFO. The design of both AFOs is shown in Figure 3.14 and Figure 3.15.